Journal of Macromolecular Science, Part A
Publication details, including instructions for authors and subscription information:
http://www.informaworld.com/smpp/title~content=t713597274

Material Design in Poly(Lactic Acid) Systems: Block Copolymers, Star Homo- and Copolymers, and Stereocomplexes

M. Spinu[a]; C. Jackson[a]; M. Y. Keating[a]; K. H. Gardner[a]
[a] DuPont Central Research and Development Experimental Station, Wilmington, Delaware, USA

To cite this Article Spinu, M. , Jackson, C. , Keating, M. Y. and Gardner, K. H.(1996) 'Material Design in Poly(Lactic Acid) Systems: Block Copolymers, Star Homo- and Copolymers, and Stereocomplexes', Journal of Macromolecular Science, Part A, 33: 10, 1497 — 1530
To link to this Article: DOI: 10.1080/10601329608014922
URL: http://dx.doi.org/10.1080/10601329608014922

J.M.S.—PURE APPL. CHEM., A33(10), pp. 1497–1530 (1996)

MATERIAL DESIGN IN POLY(LACTIC ACID) SYSTEMS: BLOCK COPOLYMERS, STAR HOMO- AND COPOLYMERS, AND STEREOCOMPLEXES

M. SPINU,* C. JACKSON, M. Y. KEATING, and
K. H. GARDNER

DuPont Central Research and Development Experimental Station
Wilmington, Delaware 19880-0328, USA

ABSTRACT

This paper gives a general overview of several approaches we have investigated for designing new PLA-based polymers with a broad range of properties and improved processability. These approaches include: copolymerization (block and stereoblock copolymers), microstructure and architecture control, and stereocomplexation. Multiblock copolymers with alternating "soft" and "hard" segments, synthesized over a broad range of chemical compositions, show properties ranging from hard plastics to elastomers. Stereoblock copolymers with alternating amorphous and semicrystalline PLA blocks combine the advantages of PLA homopolymers (crystallinity) and random copolymers (processability). Independent control of polymer architecture and microstructure allows for the synthesis of star polymers with various arm morphologies. A new method for stereocomplex formation between *L*-PLA and *D*-PLA, which combines in-situ polymerization with stereocomplexation, is also described. For the synthesis of these new materials we took advantage of: 1) chirality of lactide monomer, 2) retention of configuration during polymerization, 3) living nature of the ring-opening polymerization (ROP) of lactide in the presence of active hydrogen groups such as OH and NH_2, and 4) control of the level of transesterification reactions.

INTRODUCTION

Two of the most attractive features of poly(lactic acid) (PLA) synthetic polymers are that they are easily synthesized from renewable resources, and that they are hydro- and biodegradable. The raw material for PLA, lactic acid, can be obtained via fermentation from almost any carbohydrate-rich material, but food industry by-products such as cheese whey permeate, potato peels, and corn wet milling liquor are excellent and inexpensive feedstocks. PLA degradation initially proceeds via hydrolytic cleavage of the ester bonds to give lactic acid and its low molecular weight oligomers, which are then metabolized by both soil and marine organisms.

PLA (**4**) is nominally the condensation product of the AB monomer, lactic acid (**1**). However, side reactions which accompany the high temperature and high vacuum process limit the molecular weight obtained through direct polycondensation of lactic acid to a few thousands [1, 2]. High molecular weight PLA polymers are easily attained via ring-opening polymerization (ROP) of the cyclic diester, lactide (**3**) [3–5]. The lactide monomer (LA) is produced by depolymerization of moderate molecular weight PLA oligomers (**2**) generated by direct polycondensation of the lactic acid, as summarized in Scheme 1.

The additional step required for the synthesis of high purity lactide monomer, the limited thermal stability of PLA polymers at the processing temperatures, as well as the relatively small production volume contribute to the high cost of PLA polymers. However, biocompatibility and the nontoxic nature of the degradation products make PLA materials very attractive for biomedical applications which can tolerate the relatively high cost of these polymers. It is for this reason that most research in the area has been aimed to designing materials with properties which address the specific needs for biomedical applications [6–23].

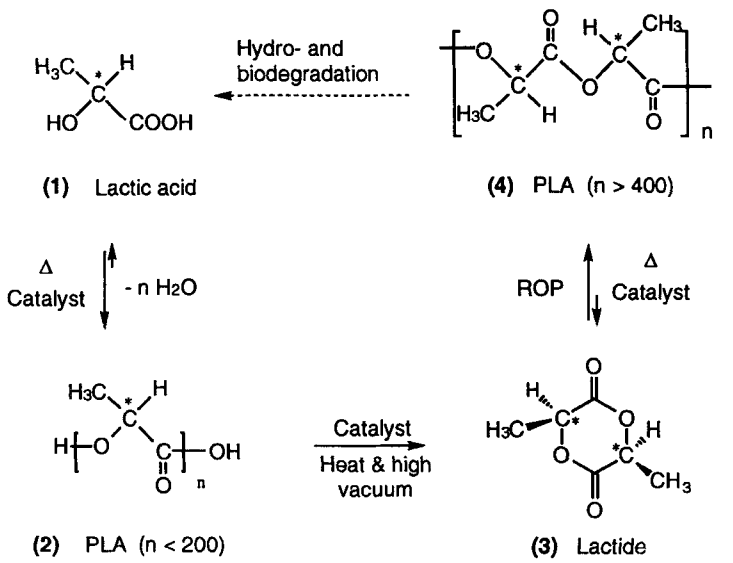

SCHEME 1. General scheme for the preparation and polymerization of lactide.

Lactide polymerization can be carried out in bulk or in solution with a variety of Lewis acid catalysts such as salts of Sn, Zn, or Ti [24, 25], Al [26–28], or rare earth metals [29–31]. Anionic catalysts such as metal alkoxides [32–34] and cationic catalysts like BF_3 and triflic acid [35, 36] have also been successfully used.

The lactide monomer contains two asymmetric carbons, hence lactide can exist as four different compounds: *L,L* and *D,D* antipodes (*L*-LA and *D*-LA, respectively), the *L,D* diastereoisomer or *meso*-lactide, and the (*L,L* + *D,D*) racemic combination of *L*-LA and *D*-LA, *rac*-lactide.

At moderate polymerization temperatures and in the presence of transterification catalysts, the ROP takes place via cleavage of the acyl—oxygen bond, with retention of configuration at the asymmetric carbon [37]. The consequence of this polymerization mechanism is that the stereochemistry of the resulting polymers is determined by the enantiomeric composition of the monomer feed. Hence, the ROP of optically pure lactide leads to stereoregular, semicrystalline PLA, while enantiomeric mixtures produce nonstereoregular, amorphous polymers.

Poly(lactic acid) homopolymers have a melting temperature $T_m \sim 175°C$, and a glass transition $T_g = 55°C$, and require processing temperatures in excess of 185–190°C. At these temperatures unzipping and chain scission reactions leading to loss of molecular weight, as well as thermal degradations, are known to occur. Consequently, PLA homopolymers have a very narrow processing window. The most widely used method for improving PLA processability is based on melting point depression by the random incorporation of small amounts of lactide enantiomer of opposite configuration into the polymer. Unfortunately, the melting point depression is accompanied by a significant decrease in crystallinity and crystallization rates.

Poly(lactic acid) homo- and copolymers have been traditionally used for biomedical applications, and most of the research in the field was generally aimed at regulating the rate of degradation in drug release systems. Much less attention was given to features which are important for general use applications such as use temperature range, melt processability, and physical-mechanical properties. For many biomedical applications where the upper use temperature is generally below the glass transition of the PLA polymers, the absence of a crystalline phase is not a significant limitation. However, for most plastics applications where higher mechanical properties are needed and the upper use temperature requirements are more demanding, the presence of a crystalline phase is critical for material performance. In this paper we describe various methods for PLA material design for improved processability without significant loss of crystallinity.

EXPERIMENTAL

Materials

Polymer grade *L*- and *D*-lactide were purchased from Purac, stored in a refrigerator, and warmed up to room temperature under an inert atmosphere before use. Tin(II) bis(2-ethylhexanoate), in short $Sn(Oct)_2$, was purchased from Sigma Chemical Co. and used as received. Inositol was purchased from Aldrich and used as received. The α-ω hydroxyl functionalized polycaprolactone (PCAP), polyethylene oxide (PEO), and polytetramethylene oxide (PTMO) were purchased from

Aldrich Co. and dried by azeotroping with toluene. Toluene was dried by refluxing over a benzophenone-sodium complex.

Polymerizations

All polymerizations were carried out in bulk under an inert atmosphere. The reactants were added to the reaction flask in a glove box under a nitrogen atmosphere, and the catalyst solution (0.1 M in dry toluene) was added via syringe through a rubber septum. Unless otherwise specified, the polymerizations were carried out at 150–160°C for 15–30 minutes following each monomer addition. Relatively low polymerization temperatures and short polymerization times were used in order to limit transesterification reactions which could ultimately lead to structure randomization. Under these polymerization conditions, no detectable randomization reactions were observed (by ^{13}C NMR). The molar ratio of monomer/catalyst was 2000/1. All polymerizations were one-pot reactions; no intermediate species were isolated in the case of multiple monomer additions or multiple step reactions. The final polymers were dissolved in methylene chloride, precipitated into an excess of hexane, filtered, and dried under vacuum to a constant weight.

Characterization

Absolute molecular weights were determined on a size exclusion chromatograph with differential refractive index, viscosity, and light-scattering detectors. The columns were 3 PL Gel linear mixed bed 10 mm packing columns, 300 mm × 7.5 mm i.d. each (Polymer Labs, Amherst MA). The detectors were concentration detector Model 410 (Waters Associates, Millford, MA), viscometer detector Model 110 (Viskotek Corp., Porter, TX), and light-scattering photometer Model F, with helium neon laser (633 nm) (Wyatt Technology Corp., Santa Barbara, CA). HPLC-grade THF was used as the mobile phase, and the temperature was 30°C. For the less soluble PLA stereocomplex, GPC analysis was carried out on a Waters instrument equipped with microstyragel column for porosity ranges of 10^5, 10^4, 500, and 100, using hexafluoroisopropanol (HFIP) solvent and a refractive index detector. DSC (differential scanning calorimetry) analyses were carried out on a DuPont model 9900 thermal analyzer at a standard heating rate of 10°C/min, samples of 5–20 mg, and a nitrogen atmosphere. Equilibrium melting temperatures and half crystallization times ($t_{1/2}$) were measured with a Perkin-Elmer DSC-7. ^{13}C-NMR spectra were acquired at RT on a 300GE spectrometer using deuterated HFIP solvent. X-ray diffraction data were collected using a Philips powder diffractometer (CuKα) symmetrical transmission with 1 degree slits.

PLA COPOLYMERS

Copolymers of *L*-LA and *D*-LA, as well as copolymers of LA with a variety of comonomers such as caprolactone and glycolide, have been extensively described in the literature [38–52]. Depending on the polymerization method and the monomer system used, both random and block copolymers have been synthesized. Simultaneous copolymerization of *L*- and *D*-LA with equal reactivities leads to random,

amorphous copolymers, while copolymerization of monomers with different reactivities such as LA and ϵ-caprolactone [47] or LA and glycolide [52] produces block copolymers with various degrees of crystallinity. The molecular weight and microstructure of PLA copolymers produced by simultaneous copolymerization depend on polymerization conditions such as catalyst type [42] or polymerization temperature [43, 44].

Synthesis of AB diblock and ABA triblock copolymers, in which A are PLA blocks and B are blocks of different chemical composition, has also been described in the literature. This synthesis is generally achieved by sequential monomer addition in a "living" polymerization process [30, 31, 33, 41, 53–55] or by using preformed oligomers containing active hydrogen end groups such as NH_2 or OH as a macroinitiator for the ROP of lactide [56–60].

"Living" polymerizations of ϵ-caprolactone (ϵ-CAP) and LA have been described for aluminum alkoxides initiators [41, 53, 54], potassium methoxide [33], (tetraphenyl-porphyrinato)Al(OR) [55], and yttrium and lanthanide alkoxides [30, 31]. In these polymerizations, ϵ-CAP must always be polymerized first, limiting this synthesis to the preparation of AB diblock copolymers.

The macroinitiator method can produce ABA triblock copolymers which can, in principle, cover a broad range of chemical compositions. In practice, however, high molecular weight ABA triblocks can only be obtained within a relatively narrow range of chemical compositions. The key limiting factor in this synthesis is the inverse dependence of molecular weight of ABA triblocks on OH concentration.

ABA Triblock Copolymers

The general scheme for the synthesis of ABA triblock copolymers using the macroinitiator approach is summarized in Scheme 2. In the systems we have investigated, the B blocks are generally OH-terminated low glass transition temperature oligomers, and the A blocks are semicrystalline PLA blocks.

In order to produce semicrystalline PLA blocks, we used lactide monomer with an enantiomeric purity $\geq 98\%$ in *L*-LA. The thermal transitions and the degree of crystallinity for a number of ABA triblocks are summarized in Table 1, and typical physicomechanical properties are summarized in Table 2. All ABA triblock copolymers show a melting temperature (T_m) and a degree of crystallinity (X_c) for the *L*-PLA blocks only slightly decreased when compared to *L*-PLA homopolymers.

The range of properties available through ABA triblock copolymers is quite limited. Even though ABA triblocks are softer plastics, as indicated by the decrease in the initial modulus with increasing B content, these copolymers remain brittle, with low elongation at break. The limited range of properties is a direct consequence of the relatively limited chemical composition range within which high molecular weight ABA triblock copolymers could be produced (0–15 wt% B component). At higher B content the molecular weights of the ABA triblock copolymers are too low to yield materials with sufficient strength for most plastics applications.

One approach to broaden the composition range while maintaining moderate molecular weights for ABA triblocks is to use a higher molecular weight B macroinitiator. Pennings and coworkers [61] described the use of difunctional rubber prepolymers with M_n = 41,000–65,000 g/mol as macroinitiators for the synthesis of triblock copolymers containing up to 34 wt% rubber. These copolymers showed

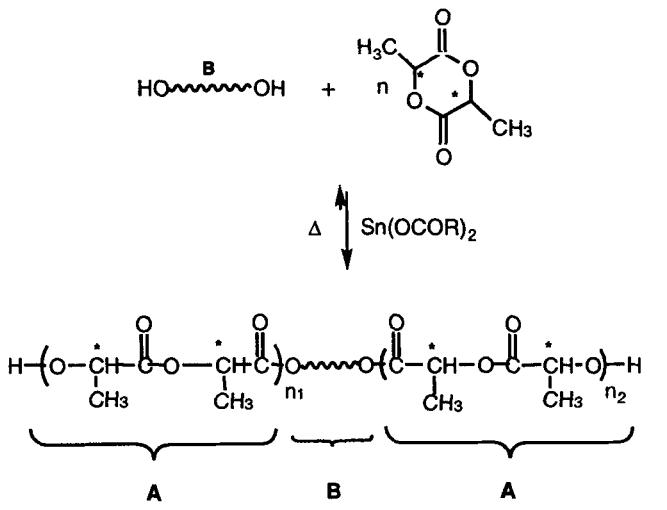

SCHEME 2. Synthesis of ABA triblock copolymers: A = PLA blocks; B = telechelic, OH-functionalized oligomers.

lower than expected molecular weight, a result which was attributed to coinitiation by trace impurities under less than the ideal conditions employed in these experiments. The very low diol concentration used in Pennings' experiments represents a significant departure from the ideal conditions for these reactions which require high concentrations of diol initiators as well as low polymerization temperatures and extremely pure monomers.

$(ABA)_n$ Multiblock Copolymers

In order to avoid the limitations associated with the synthesis of ABA triblock copolymers, one needs to control the molecular weight and chemical composition independently. We decoupled the two variables by introducing a subsequent chain

TABLE 1. Thermal Transitions and Degree of Crystallinity for ABA Triblock Copolymers (PCAP = polycaprolactone; PEO = polyethylene oxide)

Type B block	Theoretical A/B ratio, wt%	Theoretical $\langle M_n \rangle$, g/mol	T_g, °C	T_m °C	X_c,[a] %
L-PLA	100/0	>100,000	56	170	37
PCAP-2K	97/3	66.6K	52	172	32
PEO-3.4K	95/5	69.6	46	170	32
PEO-8K	88/12	58.6	48	168	32

[a]The degree of crystallinity is normalized for the content of semicrystalline component in the copolymer.

TABLE 2. Mechanical Properties[a] of ABA Triblock Copolymers

Type B block	Theoretical A/B ratio, wt%	Theoretical $\langle M_n \rangle$, g/mol	Initial modulus at maximum, kpsi	Tensile strength at break, psi	Elongation at break, %
L-PLA	100/0	—	300	9200	5.0
PCAP-2K	97/3	66.6K	278	4900	2.5
PEO-3.4K	95/5	69.6	230	4700	3.0
PEO-8K	88/12	58.6	125	2040	3.0

[a]Crosshead speed = 0.2 in./min (~5 mm/min). Each value is an average of 5 measurements. For SI units: 1 PA = 1 N/m^2 = 1.450 × 10^{-4} psi, or 1 psi = 0.69 × 10^4 Pa.

extension step to convert the ABA triblocks to high molecular weight $(ABA)_n$ multiblock copolymers [62]. The chain extension step, which takes advantage of the "living" nature of OH-initiated polymerization of LA, can be carried out using highly reactive difunctional reagents such as diisocyanates, diacyl chlorides, bicyclic compounds, etc. The two-step synthesis is schematically described in Scheme 3.

Copolymer Chemical Composition

The two-step synthesis of $(ABA)_n$ multiblock copolymers allows for the preparation of high molecular weight copolymers over a very broad range of chemical compositions. The B block is a difunctional, low glass transition temperature oligomer such as aliphatic polyesters like poly(butylene-ethylene-adipate), PBEA, and poly(caprolactone), PCAP; aliphatic polyethers like poly(ethylene oxide), PEO, and poly(tetramethylene oxide), PTMO; poly(dimethylsiloxane), PSX. The A block is a semicrystalline PLA block produced from *L*-lactide with an enantiomeric purity ≥98%.

The physicomechanical properties of these copolymers can be varied by controlling parameters such as chemical composition, the nature of the B block, and the block length. Table 3 summarizes the effect of chemical composition on copolymer properties and confirms that high molecular weight multiblock copolymers were produced for all compositions. All copolymers have a semicrystalline component arriving from the semicrystalline *L*-PLA blocks. The change in melting temperature with composition for a given B component is due to a change in *L*-PLA block

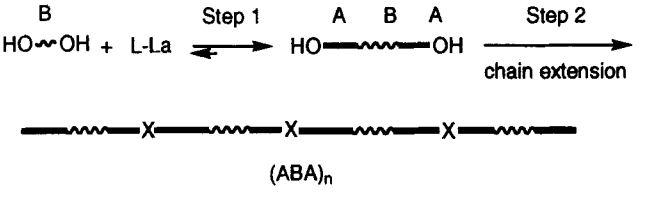

SCHEME 3. Synthesis of $(ABA)_n$ multiblock copolymers.

TABLE 3. Thermal and Mechanical[a] Properties for $[ABA]_n$ PLA Multiblock Copolymers

Nature and M_n of B block	A/B ratio, wt%	$[M_w]^a \times 10^{-3}$ g/mol	Maximum[b] tensile strength, psi	Initial[b] modulus, kpsi	Elongation[b] at break, %	T_m, °C	X_c,[c] %
PBEA: 3.4K	90/10	94	8100	190	14	168	33
	85/15	80	—	114	—	162	30
	80/20	92	6500	106	542	155	25
	75/25	214	8300	34	630	147	21
	60/40	112	8200	12	870	121	27
	50/50	150	7400	4	1100	97	20
PCAP: 2K	90/10	88	4900	175	5	163	26
	85/15	79	6400	127	344	154	21
	80/20	—	6200	92	584	142	20
	75/25	106	5500	40	685	141	22
	50/50	109	440	2	990	90	8
PEO: 3.4K	75/25	—	2500	38	470	148	15
	50/50	—	480	3	410	81	5
8K	50/50	—	1100	14	610	104	12
PTMO: 2.9K	80/20	85	7000	115	710	149	30
	60/40	111	7400	4	870	117	9
PSX: 1K[d]	90/10	70	6700	231	6	142	16
2.5K[e]	90/10	82	7300	244	8	163	24
	90/10	102	6700	200	16	161	19
	80/20	65	5830	190	7	144	19
	60/40	58	2840	56	508	113	—
Polylactide Homopolymers (reference)							
95/5 PLA	100/0	123	9200	290	5	146	15
L-PLA	100/0	>100	9200	300	5	173	37

[a] M_n from GPC, with PS standards (THF solvent, RI detector). For SI units: 1 Pa = 1 N/m^2 = 1.450×10^{-4} psi, or 1 psi = 0.69×10^4 Pa.

[b] Films used for Instron testing were solvent cast (from CH_2Cl_2) and annealed for 6 hours at 65°C. Crosshead speed = 2 in./min (~50 mm/min). Each value represents an average of 5 measurements.

[c] % X_c represents the corrected value based on % PLA (crystallizable component).

[d] PSX-1K, hydroxy alkyl-terminated.

[e] PSX-2.5K, aminopropyl-terminated.

length. A minimum PLA block length of at least 1000 g/mol (preferably above 2000 g/mol) is required in order for their crystallization to occur.

The broad range of properties accessible through the multiblock copolymer synthesis is more evident from Figs. 1 and 2 which show the change in initial modulus and % elongation at break with copolymer composition. The dramatic change in the physical-mechanical behavior of copolymers with different chemical compositions is also illustrated by the change in the slope and the shape of the stress-strain curves in Fig. 3. This figure shows the stress-strain curves for PLA homopolymer and two multiblock copolymers containing 25 and 50% PBEA–3.4K, respectively. The PLA homopolymer is a stiff and brittle material, as indicated by the high slope and the small area under the stress-strain curve. Copolymers containing intermediate levels of the B component are softer (as indicated by the lower slope) and tougher (as indicated by the increased area under the stress-strain curve). These polymers are generally characterized by the yield point, and their failure is often ductile. At higher concentrations of the B component the multiblock copolymers display elastomeric behavior, characterized by low initial modulus and exceedingly large, reversible deformations. The reversibility of their deformation is indicated by the enclosed hysteresis curve. The proper manipulation of polymer parameters allows for the synthesis of multiblock copolymers with properties ranging from hard plastics to elastomers.

The macroscopic properties of the multiblock copolymers are controlled by their morphology, which is dependent not only on copolymer composition but also on the relative polarity of the two components and their ability to microphase separate. Our preliminary DSC, DMTA, and TEM data confirm the multiphase morphology of the segmented $(ABA)_n$ copolymers. However, a detailed understand-

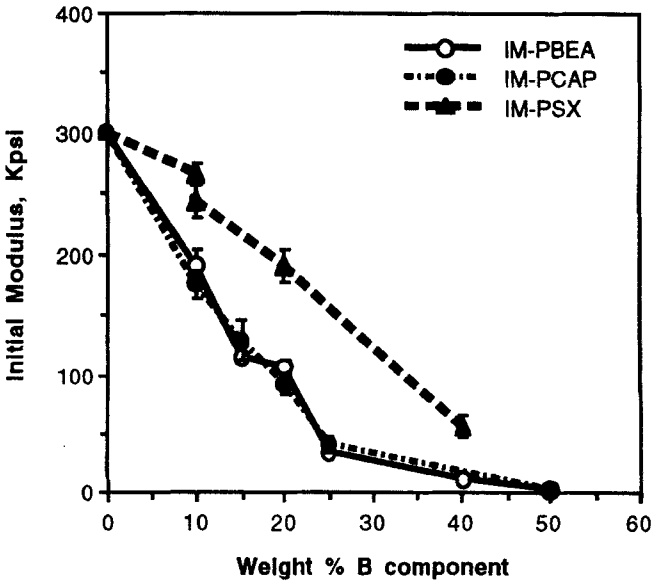

FIG. 1. Initial modulus vs composition for PLA/PBEA, PLA/PCAP, and PLA/PSX $(ABA)_n$ multiblock copolymers.

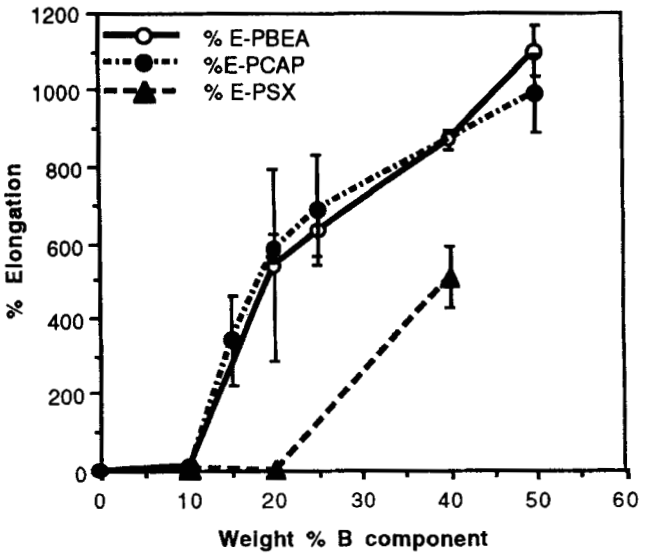

FIG. 2. Percent elongation at break vs composition for PLA/PBEA, PLA/PCAP, and PLA/PSX $(ABA)_n$ multiblock copolymers.

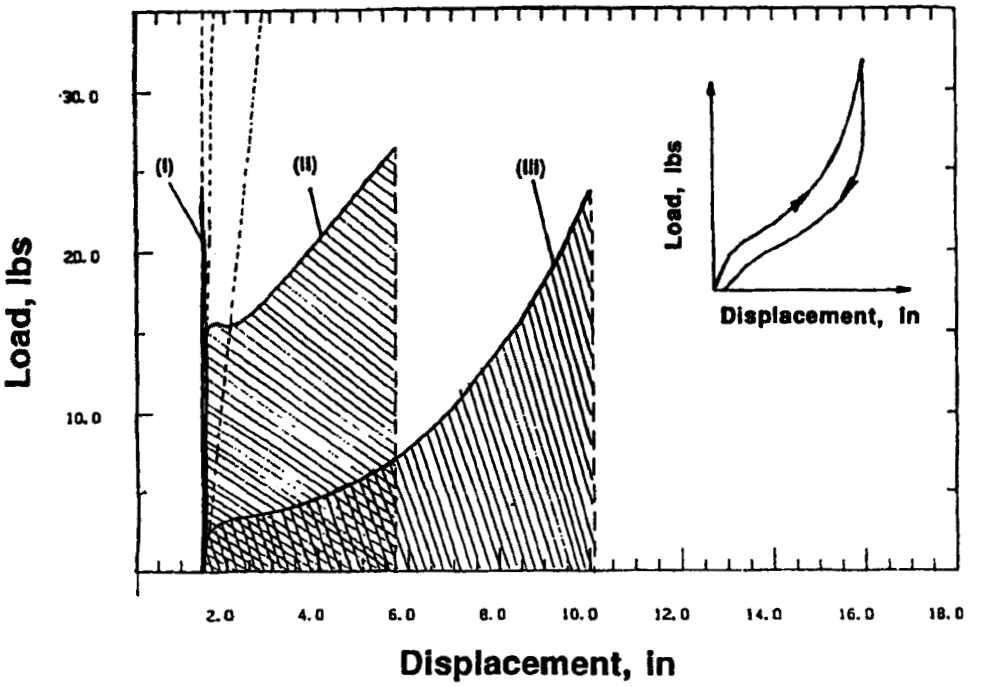

FIG. 3. Typical stress-strain curves for: (I) PLA; (II) PLA/PBEA 75/25; (III) PLA/PBEA 50/50.

ing of microphase separation and its dependence on typical system parameters such as the nature and molecular weight of the B block, chemical composition, etc. are the subjects of further studies.

PLA Stereoblock Copolymers

High molecular weight *L*-PLA or *D*-PLA homopolymers have a relatively high melting point (T_m = 175°C) and require processing temperatures in excess of 185°C. At these temperatures significant molecular weight loss as well as thermal degradation takes place. Traditionally, improved processability via melting point depression has been achieved by polymerizing an enantiomeric mixture of *L*- and *D*-lactide to generate random *L,D*-PLA copolymers. The decrease in the melting point of random *L,D*-PLA copolymers is unfortunately accompanied by a considerable decrease in the degree of crystallinity and crystallization rates, which can limit the range of applications for random copolymers. In order to decouple these parameters we synthesized PLA stereoblock copolymers in which stereoregular, semicrystalline *L*-PLA blocks (SX_c) alternate with nonstereoregular, amorphous *L,D*-PLA blocks (*A*) [63], as shown schematically in Scheme 4. Such copolymers combine the lower melting temperature characteristic to random *L,D*-PLA copolymers and the crystallization behavior characteristic to stereoregular *L*-PLA homopolymers.

Synthesis

Stereoblock copolymers were synthesized by sequential monomer addition and by controlling the enantiomeric composition of the monomer feed at each addition step. This synthesis takes advantage of the chirality of the lactide monomer, the retention of configuration upon ROP, and the living nature of polymerization initiated by hydroxyl-terminated difunctional compounds. The synthesis also requires that no significant transesterification reactions involving ester bonds and leading to a change in stereosequence distribution should occur. In order to control transesterification reactions, mild polymerization conditions have been used: polymerization temperature, 150°C; polymerization time, 15 to 30 minutes at each monomer addition step; ROP catalyst, $Sn(Oct)_2$. Earlier studies by Kricheldorf and coworkers [58] also confirm the absence of significant transesterification reactions under similar polymerization conditions. Other ROP catalysts (i.e., powdered Zn [64]) have been reported to be much more active with respect to transesterification reactions.

The amorphous blocks are random copolymers of *L*- and *D*-lactide containing at least 15% of the opposite enantiomer, while the semicrystalline blocks are *L*-PLA

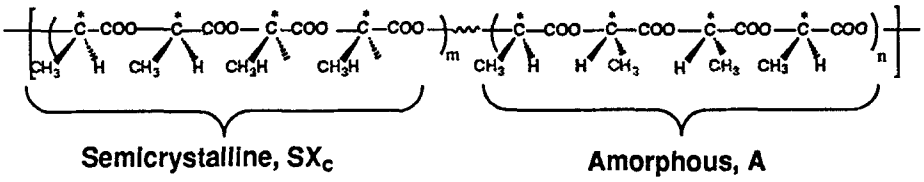

SCHEME 4. Schematic representation of PLA stereoblock copolymers with alternating semicrystalline and amorphous blocks.

homopolymers from *L*-LA with enantiomeric purity ≥98%. The stereoblock copolymers are prepared by either of two routes: route **a**, multistep monomer addition, or route **b**, two-step monomer addition followed by chain extension. This synthesis is summarized in Scheme 5.

The multistep route (**a**) is limited to a relatively low number of sequential monomer additions. Due to the equilibrium nature of the ROP, the monomer conversion at each polymerization step is incomplete (≥95%). The unreacted monomer after each step could reduce the enantiomeric purity of the fresh monomer feed for the synthesis of homopolymer blocks. To avoid such contamination, the unreacted monomer would have to be removed after each polymerization step. Route **b** controls such contamination by limiting the polymerization to two monomer additions: the OH-terminated stereo triblock copolymers $SX_c/A/SX_c$ obtained in the first two steps are chain extended to high molecular weight multiblock stereocopolymers. This synthesis allows for independent control of individual block lengths and enantiomeric composition at each addition step, as well as the overall amorphous/semicrystalline content. All these polymerizations are one-pot, melt reactions and require no isolation of the intermediate species.

The unique combination of features available through PLA stereoblock copolymers is illustrated in Fig. 4 which shows the change in melting temperature (T_m) and half crystallization time ($t_{1/2}$) for high molecular weight PLA stereoblock copolymers as a function of semicrystalline *L*-PLA block length. The melting temperature increases as the block length increases, similar to T_m dependence on molecular weight in PLA homopolymers. The half crystallization times measured at 115°C show a sudden decrease for block lengths between 10K and 15K, suggesting that at this block length the semicrystalline blocks could undergo microphase separation from the surrounding amorphous blocks. The melting temperature of these stereoblock copolymers is significantly lower than that of high molecular weight homopolymers (155 vs 175°C), while their crystallization behavior is closer to that of homopolymers. This behavior is really remarkable if we consider that the overall enantiomeric composition of these stereoblock copolymers is 87/13 *L*/*D*-lactide,

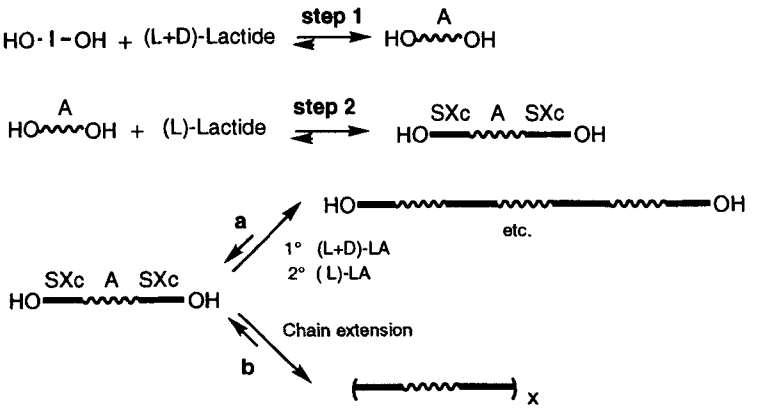

SCHEME 5. Schematic representation of the synthesis of poly(lactic acid) stereoblock copolymers.

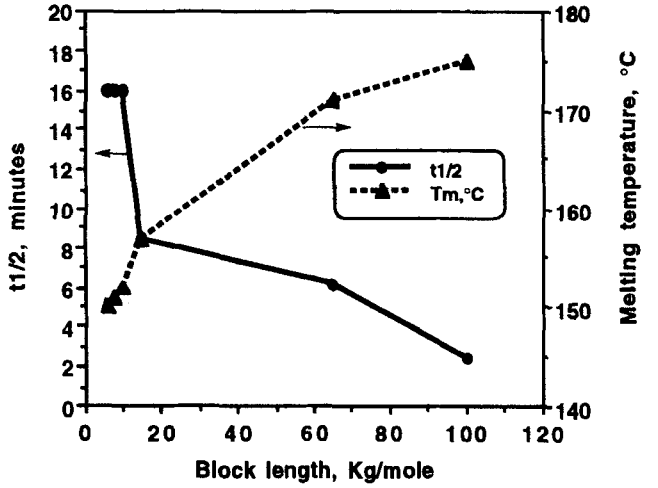

FIG. 4. T_m and $t_{1/2}$ for high molecular weight PLA stereoblock copolymers as a function of semicrystalline block length.

and that random copolymers with the same composition are completely amorphous.

PLA STAR POLYMERS

Star polymers synthesized by ROP of lactide or other lactone monomers in the presence of multifunctional hydroxyl initiators [65–68] or by the "arm-first" method [69] have been recently reported in the literature. In this paper we report the use of an additional level of versatility for the synthesis of PLA star polymers which involves simultaneous topology and microstructure control [70]. The star topology was achieved via multifunctional initiator approach, and the desired microstructure via sequential monomer addition and control of the enantiomeric composition of the monomer feed. The lack of a formal termination reaction in the OH-initiated polymerizations allows for direct initiation of a new block sequence upon new monomer addition. The initiator used in this synthesis was prepared from inositol and a mixture of 85/15 *L*/*D*-LA (using a lactide/OH molar ratio = 5/1). This mixture was equilibrated for >24 hours at 150°C, in the presence of $Sn(Oct)_2$ catalyst, to give a low molecular weight, amorphous OH-hexafunctional PLA oligomer which is readily soluble in lactide melt.

PLA Star Polymers

Random *L*,*D*-PLA copolymer stars were synthesized via single monomer addition using an enantiomeric *L*/*D*-LA mixture with ≥15% *D*-LA. These polymers are fully amorphous. Semicrystalline *L*-PLA homopolymer stars were synthesized through single monomer addition, using *L*-LA or *D*-LA with an enantiomeric purity ≥98%. Stereoblock star copolymers, with segmented amorphous and semicrystalline PLA blocks within each arm, were synthesized by a sequential monomer addi-

tion and by controlling the L/D enantiomeric composition of the lactide feed at each addition step. The synthesis of star polymers with various microstructures is summarized in Scheme 6.

Linear PLA Polymers—Controls

Linear PLA polymers of similar microstructure and overall molecular weights as the star polymers previously described were synthesized as controls. The linear polymers were synthesized through a similar synthetic approach as described for star polymers, except that a difunctional initiator was used in place of the multifunctional initiator. The schematic representation of the star/linear polymer pairs synthesized for this study is given in Scheme 7, and the corresponding enantiomeric compositions and molecular weights are summarized in Table 4.

Solution Properties

Molecular Weight and MWD

Figure 5 shows typical GPC traces for star PLA polymers prepared by the two-step monomer addition, before and after fractionation. The crude polymers show bimodal molecular weight distribution. The low molecular weight fraction attributed to coinitiation by trace impurities or heterogeneous initiation represents 15–25 wt%. For studies of dilute solution properties, the star polymers were fractionated by preparatory scale GPC to remove the low molecular weight fraction.

Mark–Houwink Coefficients and Branching Factors

For a given polymer and solvent system at a specified temperature, the intrinsic viscosity $[\eta]$ can be related to molecular weight through the following empirical equation known as the Mark–Houwink equation [71]:

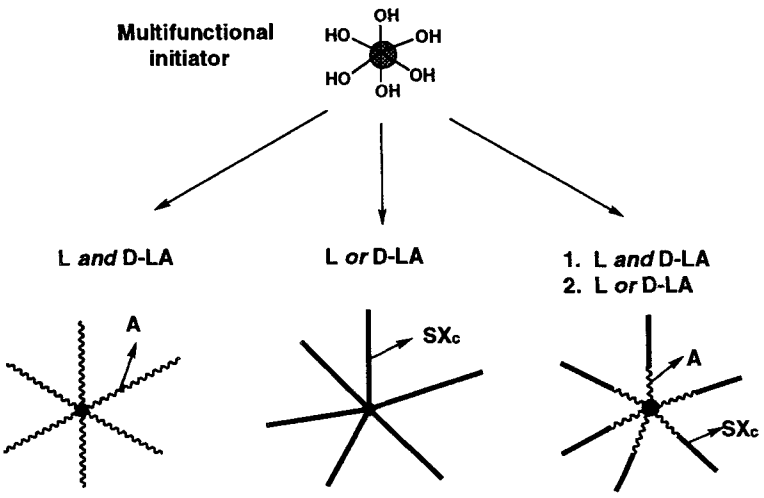

SCHEME 6. Schematic representation of the synthesis of PLA star polymers with various microstructures.

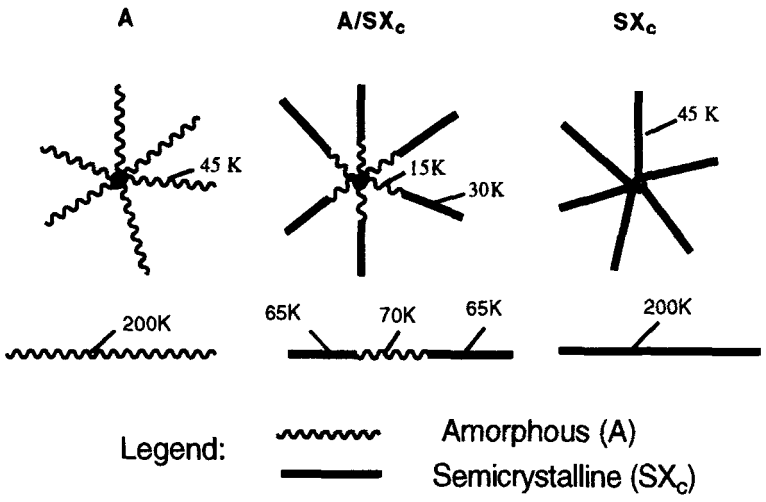

SCHEME 7. Schematic representation of PLA star polymers and the corresponding linear "controls" used in this study.

$$[\eta] = K_v M_v^a \tag{1}$$

where K_v and a are Mark-Houwink coefficients, and M_v is the viscosity-average molecular weight which lies between M_n and M_w but is usually closer to M_w. If K_v and a are known, $[\eta]$ alone will give M for an unknown polymer.

GPC with on-line light-scattering and viscosity detectors allows for both M and $[\eta]$ to be measured across the molecular weight distribution as functions of elution volume. If the polymer is sufficiently polydisperse, the Mark-Houwink coefficients, K_v and a can be determined from the intercept and slope, respectively, of a plot of log $[\eta]$ against log M. If $[\eta]$ and M are measured for both the linear and the branched polymer, one can determine a branching factor g' [72] defined as the ratio of the intrinsic viscosity of the branched to the linear polymer at the same molecular weight:

TABLE 4. Characteristic Features of Linear and Star PLA Polymers Used for the Study (R = random *L*,*D*-PLA; B = block *L*/*D*-PLA)

	Overall *L*/*D* ratio, %		A/Sx_c ratio, %		Theoretical $\langle M_n \rangle$, kg/mol	
No.	Star	Linear	Star	Linear	Star	Linear
1	92/8 (R)	92/8 (R)	100/0	100/0	270	200
2	92/8 (B)	92/8 (B)	33/77	33/77	270	200
3	100/0	100/0	0/100	0/100	270	200

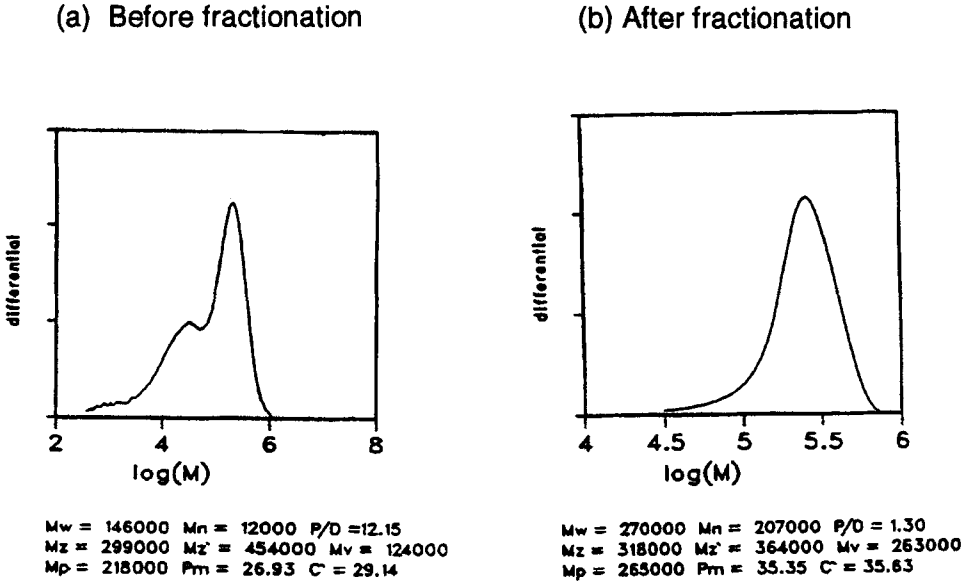

FIG. 5. Typical GPC traces for 6-arm PLA star polymers (THF solvent, PS standards, RI detector).

$$g' = \left(\frac{[\eta]_{br}}{[\eta]_l}\right)_M \tag{2}$$

The branching factor g' is related to g ($g' = g^{\epsilon}$) which is the ratio of the mean square radius of gyration of the branched polymer to that of a linear polymer of the same molecular weight [72]:

$$g = \left(\frac{<R_g^2>_{0,br}}{<R_g^2>_{0,l}}\right)_M \tag{3}$$

The ratio g is related to the number of arms, f. For star polymers with branches having a most probable molecular weight distribution (MWD), g has been shown to be related to f by the following empirical equation [72]:

$$g = \frac{6f}{(f + 1)(f + 2)} \tag{4}$$

Figures 6 through 8 show Mark-Houwink plots for PLA polymer pairs summarized in Table 4 and measured in THF solvent at 30°C. Within each polymer pair, the star and linear polymers have similar microstructures and cover approximately the same molecular weight range. It is evident that for all three pairs the dilute solution viscosities of star polymers are lower than that of the corresponding linear polymers of similar molecular weights, confirming the branched architecture.

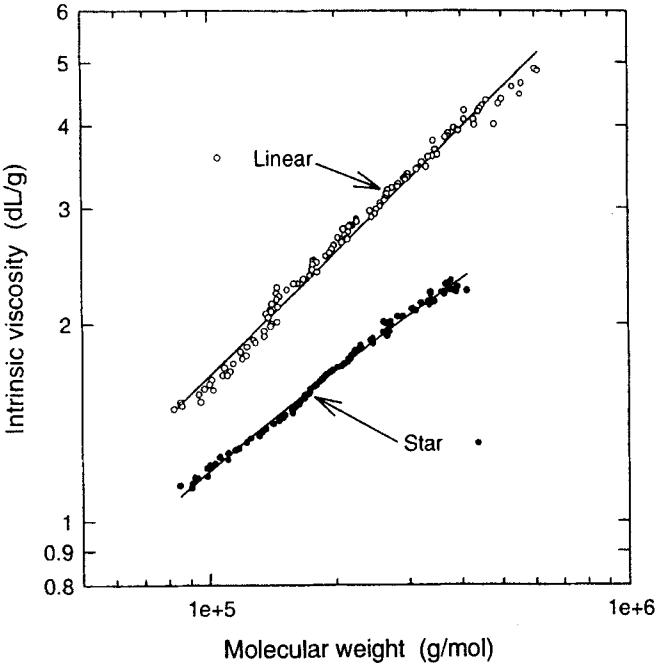

FIG. 6. Mark-Houwink plots for star and linear amorphous PLA.

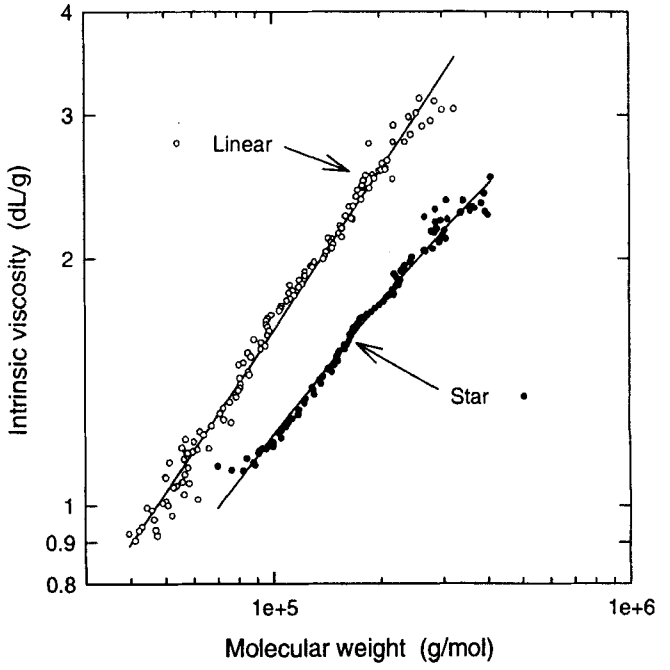

FIG. 7. Mark-Houwink plots for star and linear amorphous/semicrystalline PLA.

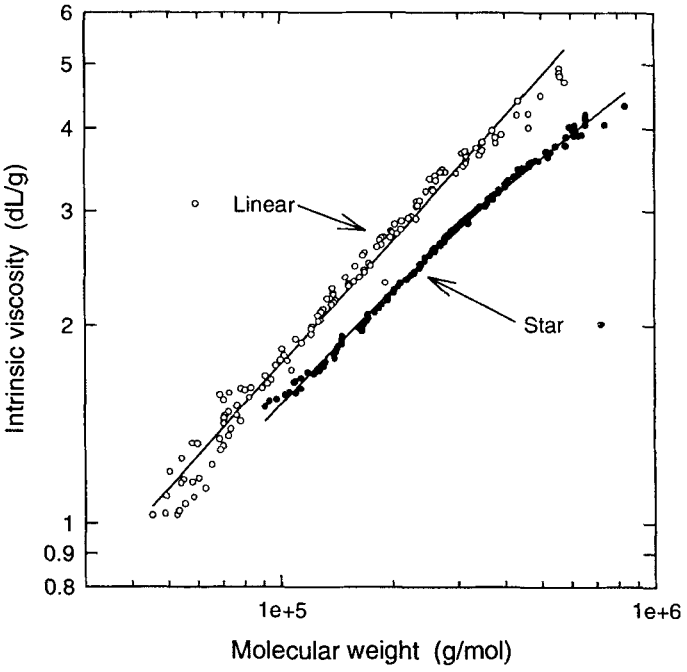

FIG. 8. Mark-Houwink plots for star and linear semicrystalline PLA.

The Mark-Houwink coefficients calculated from the logarithmic plots are shown in Table 5 and compared to the literature values for semicrystalline *L*-PLA and amorphous *L,D*-PLA measured in chloroform at 25°C [73]. Usually, the values for *a* coefficients lie between 0.5 for a theta solvent to about 0.8 for a good solvent [71]. Chloroform is known to be a good solvent for poly(lactic acid)s, and this is

TABLE 5. Mark-Houwink Coefficients for PLA/THF System at 30°C: A, A/SX_c, and SX_c Pairs of Star and Linear PLA Polymers

	Star PLA		Linear PLA	
	$K \times 10^3$	a	$K \times 10^3$	a
A	3.0	0.52	0.64	0.68
A/SX_c	2.9	0.52	0.85	0.66
SX_c	2.7	0.55	1.0	0.65
L,D-PLA (A)[a]	—	—	0.22	0.77
L-PLA (SX_c)[a]	—	—	0.55	0.73

[a]From Ref. 73 for PLA/chloroform system at 25°C.

reflected in the values of a coefficients close to 0.8 reported for the PLA/chloroform systems. The a values for PLA/THF systems were found to be lower, consistent with the fact that THF is not as good a solvent. For the linear PLA polymers, a coefficient decreases in the order $A > A/SX_c > SX_c$, which parallels the order of decreasing solubility. The linear polymers seem to be more sensitive to solvent quality when compared to star polymers of similar microstructures and molecular weights, as suggested by the range of a values observed for various microstructures.

The number of arms was calculated using Eq. (2) and (4) and selecting three values for the ϵ coefficient (0.6, 0.7, and 1.0 respectively; the ϵ values recommended for star polymers under theta conditions are 0.6–0.7 [72]). These calculations, summarized in Table 6, generally overestimate the number of arms, a departure from the theoretical value which could be attributed to nontheta conditions under which these measurements were carried out. The number of arms calculated for the star polymers decreases in the order $A > A/SX_c > SX_c$. The observed order could be attributed to the low polymerization temperatures employed in this study (150°C) and the potential for heterogeneous initiation which increases with increased semicrystalline component in the polymer.

Bulk Properties

Various bulk properties of star polymers were measured on unfractionated polymers which contain between 15 and 25 wt% of a low molecular weight component, as indicated in the GPC trace in Fig. 6.

Polymer Crystallinity

X-ray diffraction patterns for the A, A/SX_c, and SX_c PLA stars were obtained on solvent-cast polymer films annealed at 60°C for 8 hours, and are shown in Figs. 9–11. A comparison of diffraction patterns in Figs. 9 and 10 confirms the stereoblock microstructure produced by sequential monomer addition. The two polymers have the same topology and the same enantiomeric composition (92/8 L/D-lactide); however, they differ in their microstructures. While the L,D-PLA star in Fig. 9, synthesized via simultaneous copolymerization of 92/8 L/D-lactide mixture, is a random, amorphous copolymer, the star in Fig. 10, synthesized via sequential monomer addition, is a stereoblock copolymer. The corrected crystallinity index (C.I.) of the stereoblock PLA star in Fig. 10 is 36%, slightly lower than that of the semicrystalline homopolymer L-PLA (C.I. = 45%) in Fig. 11. These data are sum-

TABLE 6. Experimental g' Values and Calculated Number of Arms (f) for ϵ = 0.6, 0.7, and 1.0

		Number of arms, f		
	g'	$\epsilon = 0.6$	$\epsilon = 0.7$	$\epsilon = 1.0$
A	0.66	8.8	7.6	5.8
A/SX_c	0.70	7.6	6.7	5.2
SX_c	0.81	5.2	4.7	3.9

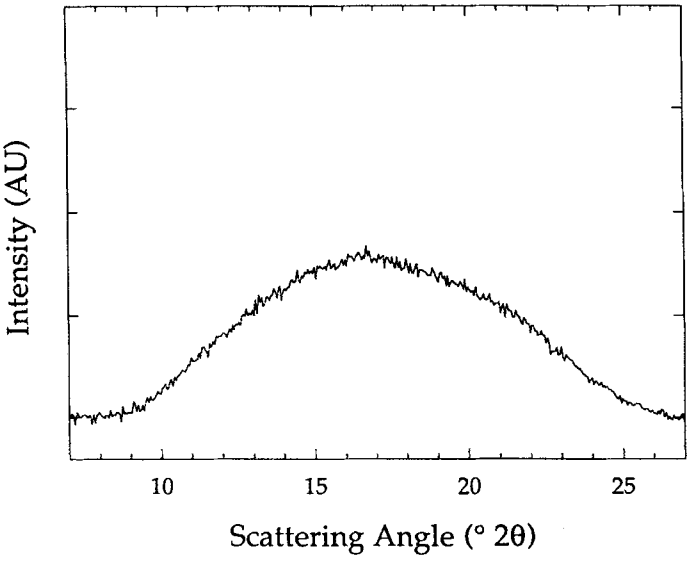

FIG. 9. X-ray diffraction patterns for amorphous PLA stars.

marized in Table 7. The corrected crystallinity index was calculated by taking into account that semicrystalline blocks represent 66% of the A/SX_c PLA copolymers. The lower crystallinity index of the stereoblock stars could be attributed to the effect of the neighboring amorphous blocks on the crystallization of stereoregular blocks, to possible contamination of the enantiomerically pure lactide by the unre-

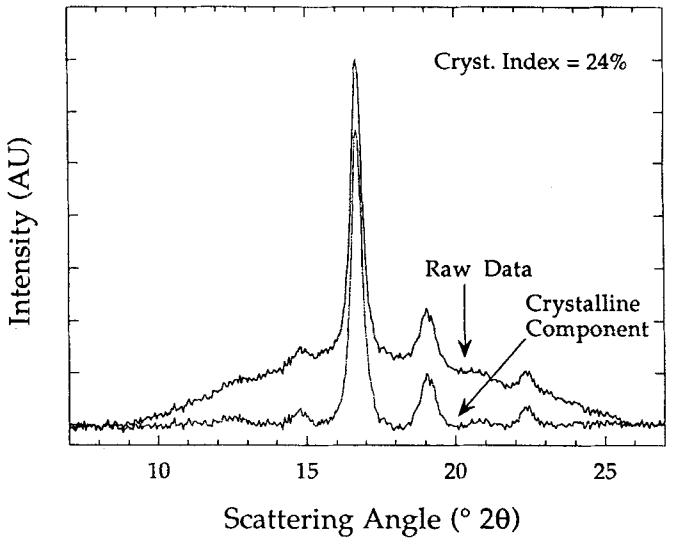

FIG. 10. X-ray diffraction patterns for amorphous/semicrystalline PLA stars.

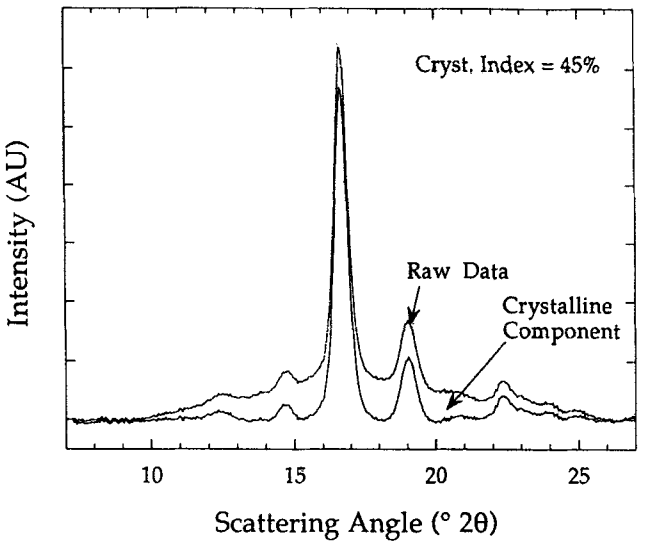

FIG. 11. X-ray diffraction patterns for semicrystalline PLA stars.

acted monomer of opposite configuration from the previous addition, or to transesterification reactions. The effect of such individual factors on the crystallization behavior or stereoblock star copolymers has not been investigated at this time.

Equilibrium Melting Temperatures

The equilibrium melting temperature, T_m^0, of a crystalline polymer is the temperature at which perfect crystals formed from infinite molecular weight chains are in equilibrium with the liquid state [71]. For chains of finite molecular weight, morphological complexities and kinetic restrictions on the crystallite dimensions make the direct determination of the equilibrium melting point virtually impossible, and indirect methods are usually used. One such method is the Hoffmann-Weeks extrapolation technique [74] in which melting temperature T_m is measured as a function of crystallization temperature T_c, and the plot T_m vs T_c is extrapolated to the intersection with the straight line $T_m = T_c$ to give the equilibrium melting temperature, T_m^0.

TABLE 7. Percent Crystallinity (X_c) for PLA Stars of Various Microstructures (R = random *L,D*-PLA copolymer; B = *L/D*-PLA stereoblock copolymer)

No.	*L/D* ratio, %	A/SX_c ratio, %	C.I., %
1	92/8 (R)	100/0	–
2	92/8 (B)	33/77	24 (36)
3	100/0	0/100	45

The experimental procedure involved heating the polymers above their melting temperature in order to erase the thermal history, then quenching the sample (at 300°/min) to the desired crystallization temperature, T_c, to carry out the isothermal crystallization for the desired length of time. The melting temperatures, T_m, were measured as the end of the melting endotherm on the subsequently heated samples. T_m values were plotted against T_c, and the equilibrium melt temperatures, T_m^0, were determined as shown in Fig. 12.

The increase of T_m per 10°C increase of T_c ($\Delta T_m/\Delta T_c$) provides additional information on the polymer crystallizability. These values are 3.6 for the "amorphous" stars (1), 1.1 for the segmented A/SX_c stars (2), and approximately 0 for the SX_c stars (3), indicating that the crystal perfection increases in the order $A < A/SX_c < SX_c$, as expected.

Half-Crystallization Times

The half-crystallization times ($t_{1/2}$) were measured at various crystallization temperatures, and the effect of topology and microstructure investigated. The equilibrium melting temperatures and the crystallization half times are summarized in Table 8.

The topology effect on crystallization rate is evident when $t_{1/2}$ of star and linear PLA polymers of similar microstructures and molecular weights are compared. Figure 13 shows these data for semicrystalline *L*-PLA homopolymers. The star polymers show 1.3–1.5 times shorter $t_{1/2}$, at all three crystallization temperatures, when compared to the corresponding linear polymers. This behavior may be partly a molecular weight effect: the individual arm in PLA stars is much shorter (45K) than the overall chain length in linear PLA (~ 200K).

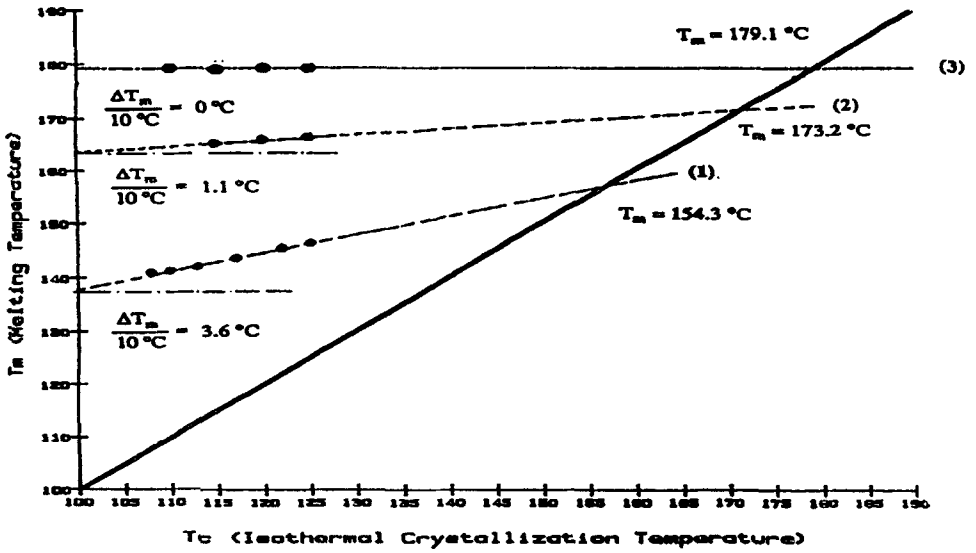

FIG. 12. Equilibrium melt temperature (Hoffman–Weeks extrapolation) for PLA stars with various microstructures: (1) A; (2) A/SX_c; (3) SX_c.

TABLE 8. Equilibrium Melting Temperatures (T_m^0) and the Crystallization Half Times ($t_{1/2}$) for Star PLA Homo- and Copolymers

L/D ratio, %	$t_{1/2}$ (T_c = 115°C), minutes	$t_{1/2}$ (T_c = 120°C), minutes	$t_{1/2}$ (T_c = 125°C), minutes	T_m^0, °C
92/8 (A)	–	–	–	154[a]
92/8 (A/SX_c)	4.4	8.5	16.9	173
100/0 (SX_c)	1.7	2.4	4.8	179

[a]Very weak melting transition (<2% crystallinity).

The microstructure effect on crystallization rate was estimated by comparing $t_{1/2}$ of star PLA polymers of similar molecular weights but different microstructures. Figure 14 summarizes $t_{1/2}$ values for SX_c and A/SX_c stars at three different crystallization temperatures. The $t_{1/2}$ for segmented A/SX_c stars is 2.6–3.5 times longer than that of SX_c homopolymer stars.

While further studies are needed to understand the individual contributions of various parameters to solution and bulk polymer behavior, a combination of topology and microstructure control provides a versatile tool for the synthesis of PLA materials with a broad range of rheological and crystallization behavior.

PLA STEREOCOMPLEX

Stereocomplexation between optically active polymers, *D*-polymer and *L*-polymer, has been reported for many polymer pairs [76–86]. Polymeric stereocomplex between *L*-PLA and *D*-PLA was first reported by Ikada et al. [87]. Since then,

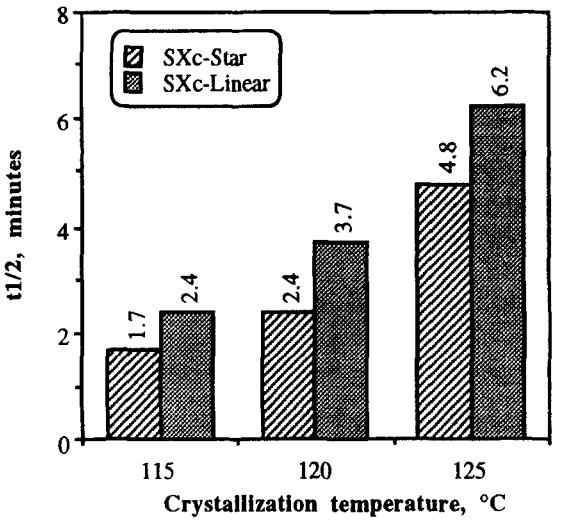

FIG. 13. Effect of topology on half crystallization times ($t_{1/2}$): linear and star semicrystalline (SX_c) PLA.

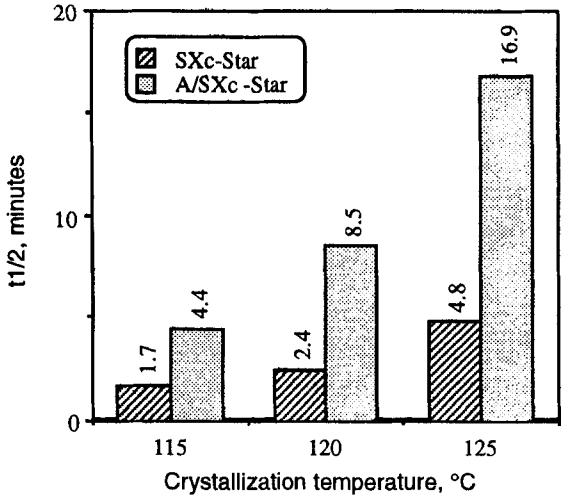

FIG. 14. Effect of microstructure on half crystallization times ($t_{1/2}$): SX_c homopolymer and A/SX_c stereoblock copolymer stars.

many studies were carried out to elucidate the conditions affecting stereocomplexation from *L*-PLA/*D*-PLA solution or melt blends [88–100], and the structure of the stereocomplex [94–97, 101].

The PLA stereocomplex consists of racemic crystalline structures in which *L*-PLA and *D*-PLA chains are packed side by side, with a 1:1 ratio of *L*:*D* monomer units [101]. It has been shown that upon stereocomplex formation the chain conformation changes from 10_3 to 3_1 helix [101, 102]. According to conformational models [102], the major difference between the two helical forms is that in the 3_1 conformation the helix winds a little tighter, going from 108 to 120° rotation per residue. The relatively small conformational change produces a dramatic change in the molecular shape (this kind of difference is often seen when the projections of integral and nonintegral helices are compared). The 10_3 helix when projected down the chain axis is truly rodlike, while the comparable projection of the 3_1 helix has "bumps" and "hollows," as shown in Scheme 8. As a result, the chain-to-chain separation distance in the 3_1 helical structure is 0.4 Å smaller than that found for the 10_3 helices.

One of the consequences of tighter packing in the stereocomplex is the increased resistance to hydrolysis, which results in lower in-vivo and in-vitro degradation rates. This is a very attractive feature for applications in which biodegradable materials with a long lifetime are needed (such as resorbable biomedical implants). Another consequence of the tighter packing in the stereocomplex is its increased melting temperature when compared to the enantiomerically pure polylactides from which the blends are prepared (225 and 175°C, respectively). The high melting temperature of *L*-PLA/*D*-PLA stereocomplex makes its melt processing nearly impossible.

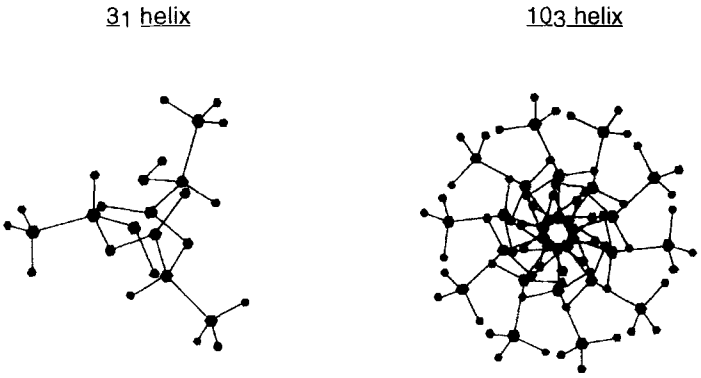

SCHEME 8. Molecular conformation for 3_1 and 10_3 PLA helix projection down the chain axis.

New Method for Stereocomplex Formation

Stereocomplexation of *L*-PLA and *D*-PLA has been previously achieved from enantiomeric polymer blends prepared by solution or high temperature melt blending of the two polymers. Here we describe a new approach to stereocomplex formation which combines polymerization with stereocomplexation and eliminates the need for solvent or high temperature blending of the two polymers [103, 104]. In this approach the preformed PLA of one of the enantiomers (for example, *D*-PLA) is dry-blended with an equimolar amount of lactide monomer of the opposite configuration (*L*-LA) and a polymerization catalyst. When the mixture is heated above 100°C the lactide monomer melts and at least partially dissolves the initially present *D*-PLA polymer, forming an intimate monomer/polymer blend. Upon further heating, *L*-LA will polymerize to generate poly-*L*-lactide in situ, and in close proximity with poly-*D*-lactide. We found that under these conditions the stereocomplex is formed in situ as the polymerization proceeds. This process is schematically described in Scheme 9.

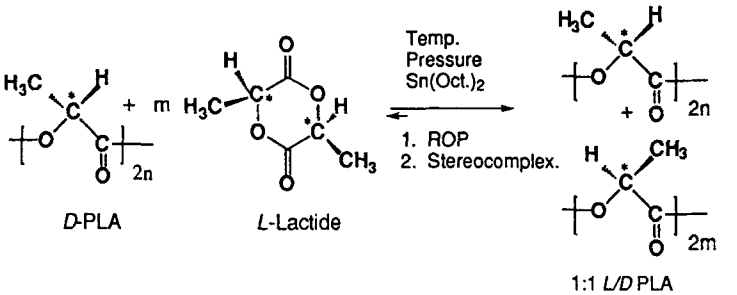

SCHEME 9. Stereocomplex formation during polymerization of *L*-LA in the presence of *D*-PLA.

The polymerization can be carried out at temperatures as low as 140–150°C, hence the conformational change from 10_3 to 3_1 helix could be accomplished at temperatures below the melting of either the homocrystals or racemic crystals, and with no solvent present. Furthermore, if the polymerization is carried out under pressure, the stereocomplex can be consolidated into finished or semifinished parts which can be machined into the desired shape. This forming method eliminates the need for high temperature processing of the high melting stereocomplex which would lead to severe thermal degradation.

In order to learn about the transformations taking place during heating of enantiomeric monomer/polymer blends, we used pressure-volume-temperature (PVT) experiments for in-situ monitoring. These measurements were carried out in a 1.0-cm^3 dilatometer-type PVT apparatus using isobaric thermal expansion conditions. In a typical experiment a 50:50 mixture of *L*-LA and *D*-PLA containing $Sn(Oct)_2$ catalyst (2000:1 LA/catalyst) were charged into the PVT cell and heated from RT to 230°C, with a hold-up time of 1–3 hours between 140 and 170°C, to carry out the polymerization. Figure 15 shows specific volume changes versus temperature for a PVT experiment in which the polymerization was carried out at 160°C for 2 hours.

In the absence of phase transitions, a monotonous increase in specific volume with temperature, due to thermal expansion, is observed. Discontinuities in specific

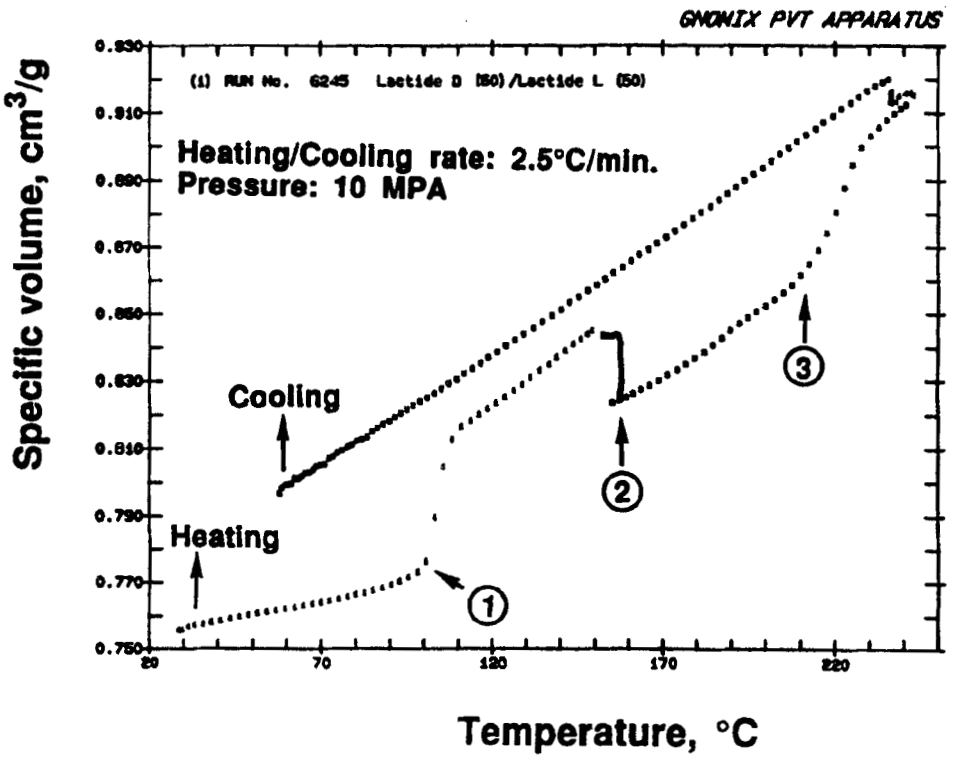

FIG. 15. Typical PVT measurements: specific volume versus temperature during isobaric (10 MPa) heating and cooling (2.5°C/min) of an equimolar mixture of *L*-LA/*D*-PLA.

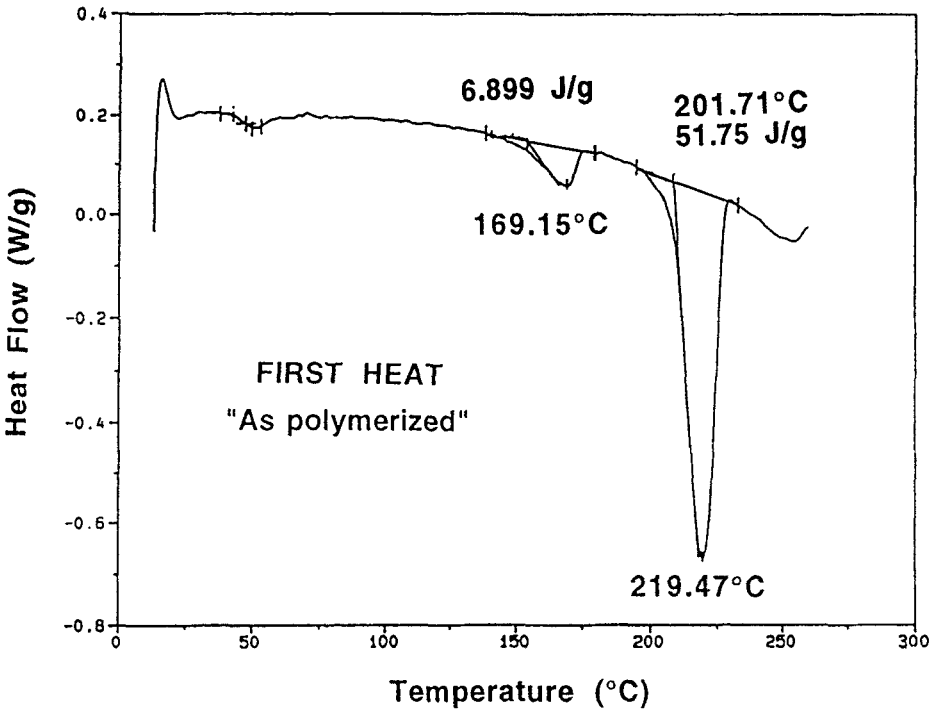

FIG. 16. DSC thermogram for "as polymerized" *L/D*-PLA stereocomplex. Heating rate: 10°C/min; nitrogen atmosphere.

volume changes indicate that the sample is undergoing a phase transition. The three major discontinuities in the specific volume–temperature curve in Fig. 15 are associated with the following transformations: (1) Melting transition of lactide monomer at approximately 100°C; (2) Polymerization of LA, followed by crystallization of PLA, at ~160°C; (3) Polymer melting at approximately 220°C (characteristic to *L/D*-PLA stereocomplex). A very weak transition, corresponding to the melting transition of PLA single enantiomer, is also observed around 160–170°C. This experiment demonstrates that in-situ polymerization is accompanied by stereocomplexation and that PLA racemic crystals are formed in preference to PLA homocrystals. The cooling cycle, carried out at a constant cooling rate of 2.5°C/min, shows no recrystallization, indicating that stereocomplex formation from the racemic *L*-PLA/*D*-PLA melt is slow. The "as-polymerized" polymers were characterized by TGA, DSC, SAXS, ^{13}C NMR, and GPC.

Thermal Analysis

Dynamic TGA analysis indicates high conversion of monomer to polymer ($\leq 3\%$ residual lactide). DSC analysis indicates that the "as-polymerized" *L/D*-PLA material has a major melting transition around 220°C, corresponding to the stereocomplex component. A minor melting transition at 160–170°C indicates the presence of a small amount of PLA homocrystals in the "as-polymerized" material. A typical DSC is shown in Fig. 16.

X-Ray Diffraction

In-situ stereocomplex formation under the conditions described in this paper is also evident from x-ray diffraction patterns. Plots of the density of the scattered beam against the angle of incidence are shown in Fig. 17 for "as-polymerized" *L/D* PLA stereocomplex (B) and two controls: (A) the stereocomplex prepared by physical blending of *L*-PLA and *D*-PLA and followed by annealing at 190°C, and (C) *L*-PLA single enantiomer. According to x-ray diffraction patterns, the stereocomplex is the major component in the "as-polymerized" material while the homopolymer crystals represent a small percentage of the crystalline phase. These data are in good agreement with the DSC results.

^{13}C NMR

One of our concerns regarding in-situ polymerization/stereocomplexation method was the potential for transesterification reactions which could lead to undesirable microstructure randomization. To prevent these undesirable effects, mild polymerization conditions were employed for the stereocomplex preparation. Figure 18 shows the carbonyl region of the ^{13}C-NMR spectra (hexade sequences [105]) for: (a) *L*-PLA/*D*-PLA stereocomplex, and (b) racemic (*L* + *D*)-PLA. It is evident that under the conditions used for stereocomplex preparation, no significant randomization has occurred.

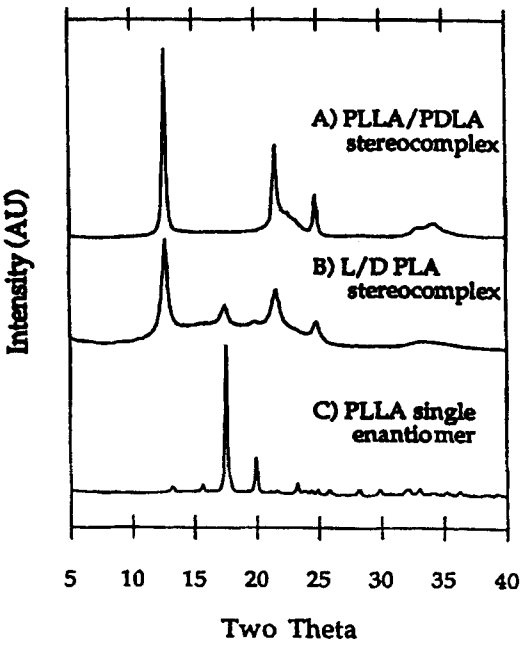

FIG. 17. X-ray diffraction patterns for: (A) *L*-PLA/*D*-PLA stereocomplex from polymer blends; (B) "as polymerized" *L/D*-PLA stereocomplex by in-situ polymerization/stereocomplexation; (C) *L*-PLA homopolymer.

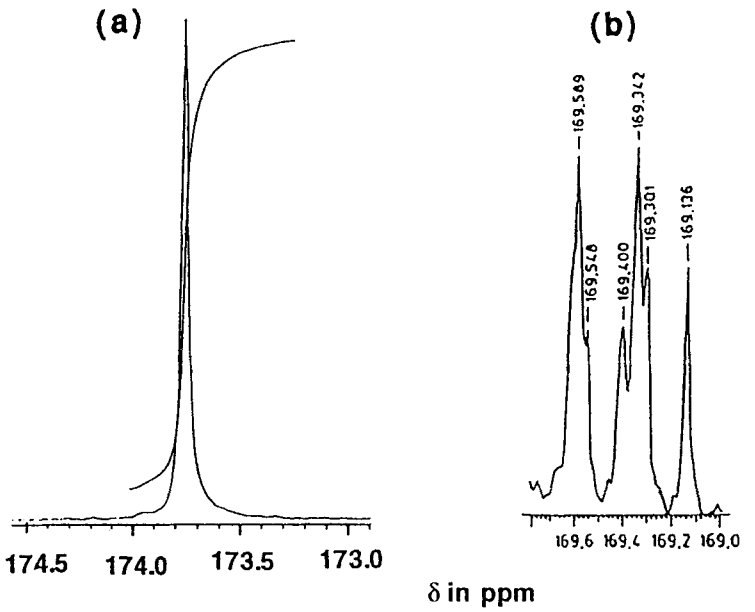

FIG. 18. ^{13}C NMR for carbonyl region (hexade sequences) for (a) *L/D*-PLA "as polymerized" stereocomplex, and (b) *L,D*-PLA random copolymer from racemic lactide.

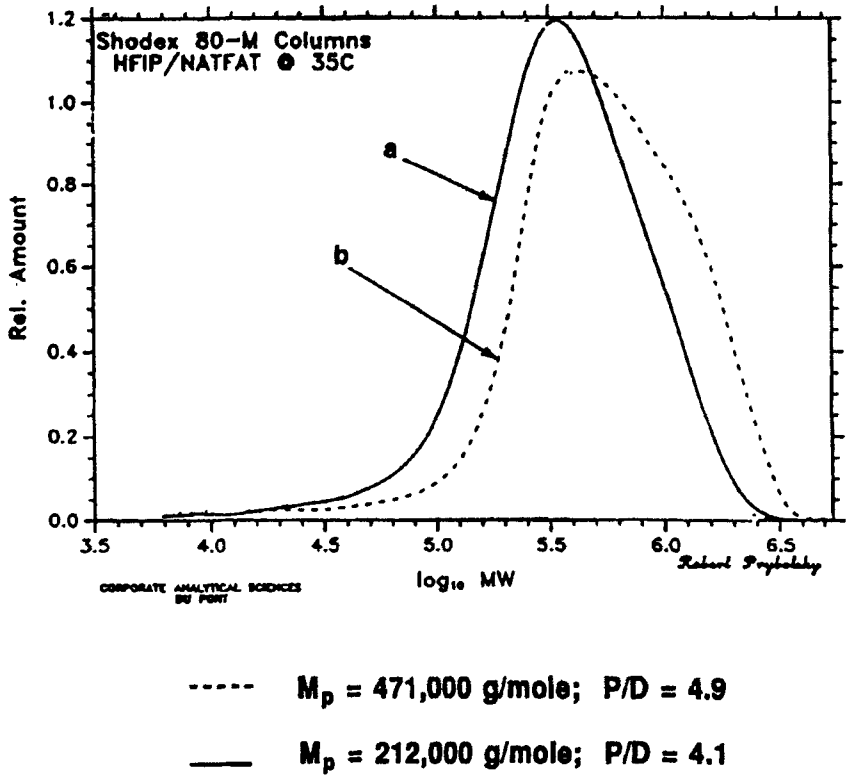

FIG. 19. GPC traces for: (a) *L/D*-PLA stereocomplex prepared by in-situ polymerization; (b) *D*-PLA in the initial monomer/polymer blend used for the preparation of stereocomplex (HFIP solvent, PET standards).

Molecular Weight and MWD

Figure 19 shows GPC traces for *D*-PLA in the initial monomer/polymer blend and the "as-polymerized" *L*-PLA/*D*-PLA stereocomplex prepared by in-situ polymerization of *L*-lactide in the presence of *D*-PLA and at temperatures below 170°C. The molecular weight of the "as-polymerized" stereocomplex is lower than that of the polymeric component in the initial monomer/polymer blend, suggesting that some chain redistribution of the initially present *D*-PLA polymer may have occurred. The chain redistribution was favored by the nonequilibrium molecular weight distribution of this polymer (P/D = 4.9).

CONCLUSIONS

The synthetic tools we have used in the design of new PLA polymers are not new, however, they have been greatly underutilized in the past. These synthetic tools include monomer chirality, retention of configuration through ROP, "living" nature of ROP of lactide in the presence of active hydrogen groups such as OH and NH_2, and control of transesterification reactions. We have demonstrated that by proper manipulation of these readily available tools, materials with a broad range of properties and improved processability could be produced. In addition, we reported a low temperature, solvent-free process for stereocomplex formation between *L*-PLA and *D*-PLA. The examples described in this review represent but a few of many opportunities for material design in PLA-based systems.

ACKNOWLEDGMENTS

We thank Dr. David Walsh for PVT experiments and valuable discussions, Dr. Howard Barth for GPC fractionation, Mr. Robert Pribolski for GPC measurements, and William W. Hyde for technical assistance.

REFERENCES

[1] W. H. Carothers, G. L. Dorough, and F. J. van Natta, *J. Am. Chem. Soc., 54*, 761 (1932).
[2] H. Fukuzaki, Y. Aiba, M. Yoshida, M. Asano, and M. Kumakura, *Makromol. Chem., 190*, 2571 (1989).
[3] J. Kleine and H. H. Kleine, *Ibid., 30*, 23 (1959).
[4] T. Tsuruta, K. Matsuura, and S. Inoue, *Ibid., 75*, 211 (1964).
[5] W. Dittrich and R. C. Schulz, *Angew. Makromol. Chem., 15*, 109 (1975).
[6] J. Conn, R. Oyasu, M. Welsh, and J. M. Beal, *Am. J. Surg., 128* 19 (1974).
[7] P. H. Craig, J. A. Williams, K. W. Davis, A. D. Magoun, A. J. Levy, S. Bogdansky, and J. P. Jones, *Surg. Gynec. Obstret., 141* 1 (1975).
[8] H. Younes and D. Cohn, *Eur. Polym. J., 24* 765 (1988).
[9] D. Cohn and H. Younes, *Biomaterials, 10*, 466 (1989).
[10] X. D. Feng, C. X. Song, and W. Y. Chen, *J. Polym. Sci., Polym. Lett., 21*, 593 (1983).

[11] C. X. Song and X. D. Feng, *Macromolecules, 17*, 2764 (1984).
[12] J. M. Schakenraad, J. A. Oosterbaan, P. Nieuwenhuis, I. Molenaar, J. Olijslager, W. Potman, M. J. D. Eenink, and J. Feijen, *Biomaterials, 9*, 116 (1988).
[13] M. J. D. Eenink, J. Olijslager, J. H. M. Albers, J. K. Rieke, P. J. Greidanus, and J. Feijen, *J. Control. Rel., 6*, 225 (1987).
[14] C. G. Pitt, A. R. Jeffcoat, R. A. Zweidinger, and A. Schindler, *J. Biomed. Mater. Res., 13*, 497 (1979).
[15] C. G. Pitt, R. W. Hendren, A. Schindler, and S. C. Woodward, *J. Control. Rel., 1*, 3 (1984).
[16] T. Nakamura, S. Hitomi, S. Watanabe, K. Jamshidi, S. H. Hyon, and Y. Ikada, *J. Biomed. Mater. Res., 23*, 1115 (1989).
[17] J. W. Leenslag, A. J. Pennings, R. R. M. Bos, F. R. Rozema, and G. Boering, *Biomaterials, 8*, 70 (1987).
[18] R. R. M. Bos, G. Boering, F. R. Rozema, J. W. Leenslag, A. J. Pennings, and A. B. Verwey, *J. Oral Maxillofac. Surg., 45*, 751 (1987).
[19] A. Majola, S. Vainionpaa, P. Rokkanen, H. M. Mikkola, and P. Tormala, *J. Mater. Sci., Mater. Med., 3*, 43 (1992).
[20] S. Vainionpaa, P. Rokkanen, and P. Tormala, *Prog. Polym. Sci., 14*, 679 (1989).
[21] D. C. Tunc, *Clin. Mater., 8*, 119 (1991).
[22] M. Vert, F. Chabot, J. Leray, and P. Christel, *Makromol. Chem. Suppl., 5*, 30 (1981).
[23] M. Vert, P. Christel, H. Garreau, M. Audion, M. Chavanaz, and F. Chabot, *Polym. Sci. Technol., 34*, 263 (1986).
[24] H. R. Kricheldorf and Serra, *Polym. Bull., 14*, 497 (1985).
[25] M. Bero, J. Kasperczyk, and Z. Jedlinski, *Makromol. Chem., 191*, 2287 (1990).
[26] W. X. Cao, G. F. Lin, X. Y. Li, and X. D. Feng, *Polym. Bull., 20*, 117 (1988).
[27] P. Dubois, C. Jacobs, R. Jerome, and Ph. Teyssie, *Macromolecules, 24*, 2266 (1991).
[28] P. Vanhoorne, P. Dubois, R. Jerome, and Ph. Teyssie, *Ibid., 25*, 37 (1992).
[29] S. J. McLain and N. E. Drysdale, US Patent 5,028,667 (1991).
[30] S. J. McLain and N. E. Drysdale, *Polym. Prepr. Am. Chem. Soc., Div. Polym. Chem., 33*(1), 174 (1992).
[31] S. J. McLain, T. M. Ford, and N. E. Drysdale, *Ibid., 33*(2), 463 (1992).
[32] H. R. Kricheldorf and I. Kreiser-Saunders, *Makromol. Chem., 191*, 1057 (1990).
[33] Z. Jedlinski, W. Walach, P. Kurcok, and G. Adamus, *Ibid., 192*, 2051 (1991).
[34] P. Kurcok, J. Penczek, J. Franek, and Z. Jedlinski, *Macromolecules, 25*, 2285 (1992).
[35] H. R. Kricheldorf and R. Dunsing, *Makromol. Chem., 187*, 1611 (1986).
[36] H. R. Kricheldorf and I. Kreiser, *Ibid., 188*, 1861 (1987).
[37] E. Lillie and R. C. Schulz, *Ibid., 176*, 1901 (1975).
[38] A. C. Albertsson, A. Lofgren, and M. Sjoling, *Makromol. Chem., Macromol. Symp., 73*, 127 (1993).

[39] J. M. Vion, R. Jerome, P. Teyssie, M. Aubin, and R. E. Prud'homme, *Macromolecules, 19*, 1828 (1986).
[40] P. Vanhoorne, Ph. Dubois, R. Jerome, and Ph. Teyssie, *Ibid., 25*, 37 (1992).
[41] Ph. Dubois, I. Barakat, N. Ropson, Ph. Degee, R. Jerome, and Ph. Teyssie, *Macromol. Rep., A31*(Suppl. 6&7), 1127 (1994).
[42] E. J. Choi, J. K. Park, and H. N. Chang, *J. Polym. Sci., Part B, Polym. Phys., 32*, 2481 (1994).
[43] D. W. Grijpma, G. J. Zondervan, and A. J. Pennings, *Polym. Bull., 25*, 327 (1991).
[44] D. W. Grijpma and A. J. Pennings, *Ibid., 25*, 335 (1991).
[45] J. Kasperczyk and M. Bero, *Makromol. Chem., 192*, 1777 (1991).
[46] J. Kasperczyk and M. Bero, *Ibid., 194*, 913 (1993).
[47] M. Bero, J. Kasperczyk, and G. Adamus, *Ibid., 194*, 907 (1993).
[48] A. Nakayama, N. Kawasaki, I. Arvanitoyannis, J. Iyoda, and N. Yamamoto, *Polymer, 36*(6), 1295 (1995).
[49] T. Ashara, K. Yomashita, and S. Katayama, *Kogajo Kagaku Zasshi, 66*, 485 (1963).
[50] K. Chujo, H. Kobayashi, J. Suzuki, and S. Tokuhara, *Makromol. Chem., 100*, 267 (1967).
[51] K. Chujo, H. Kobayashi, S. Suzuki, S. Tukuhara, and M. Tenable, *Makromol. Chem., 100*, 262 (1967).
[52] H. R. Kricheldorf, J. M. Jonte, and M. Berl, *Makromol. Chem., Suppl., 12*, 25 (1985).
[53] C. Jacobs, Ph. Dubois, R. Jerome, and Ph. Teyssie, *Macromolecules, 24*, 3027 (1991).
[54] Ph. Dubois, R. Jerome, and P. Teyssie, *Makromol. Chem., Macromol. Symp., 42/43*, 103 (1991).
[55] L. Trofimoff, T. Aida, and S. Inoue, *Chem. Lett.*, p. 991 (1987).
[56] K. J. Zhu, L. Xiangzhou, and Y. Shilin, *J. Appl. Polym. Sci., 39*, 1 (1990).
[57] Y. Kimura, Y. Matsuzaki, H. Yamane, and T. Kitao, *Polymer, 30*, 1342 (1989).
[58] H. R. Kricheldorf and J. M. Haack, *Makromol. Chem., 194*, 463 (1993).
[59] Z. Jedlinski, P. Kurkov, W. Walach, and H. Janeczek, *Ibid., 194*, 1681 (1993).
[60] X. M. Deng, C. D. Xiong, L. M. Cheng, and R. P. Xu, *J. Polym. Sci., Part C, Polym. Lett., 28*, 411 (1990).
[61] D. W. Grijpma, R. D. A. Van Hofslot, H. Super, A. J. Nijenhuis, and A. J. Pennings, *Polym. Eng. Sci., 34*, 1674 (1994).
[62] M. Spinu, US Patent 5,202,413 (1993).
[63] M. Spinu, US Patent 5,270,400 (1993); M. Spinu, US Patent 5,346,966 (1994).
[64] F. Chabot, M. Vert, S. Chapelle, and P. Granger, *Polymer. 24*, 53 (1983).
[65] K. J. Zhu, S. Bihai, and Y. Shilin, *J. Polym. Sci., Part A, Polym. Chem., 27*, 2151 (1989).
[66] P. Bruin, G. J. Veenstra, A. J. Nihenhuis and A. J. Pennings, *Makromol. Chem. Rapid Commun., 9*, 589 (1989).
[67] S. H. Kim, Y.-K. Han, Y. H. Kim, and S. I. Hong, *Makromol. Chem., 193*, 1623 (1992).

[68] S. H. Kim, Y. K. Han, K. D. Ahn, Y. H. Kim, and T. Chang, *Ibid., 194*, 3229 (1993).
[69] D. Tian, Ph. Dubois, R. Jerome, and Ph. Teyssie, *Macromolecules, 27*, 4134 (1994).
[70] M. Spinu, US Patent 5,225,521 (1993).
[71] J. M. G. Cowie, in *Polymers: Chemistry & Physics of Modern Materials*, 2nd ed., Chapman & Hall, New York, NY, 1991.
[72] J. Roovers in *Encylopedia of Polymer Science and Engineering*, Vol. 2, 2nd ed., 1985, pp. 478–499.
[73] A. Schindler and D. Harper, *J. Polym. Sci., Polymer Chem. Ed., 17*, 2593 (1979).
[74] J. D. Hoffmann and J. J. Weeks, *J. Res. Natl. Bur. Stand. A, 66*, 13 (1962).
[75] J. T. Gruver and G. Kraus, *J. Polym. Sci., Part A, 3*, 105 (1965).
[76] M. Tsuboi, A. Wada, and N. Nagashima, *J. Mol. Biol., 3*, 705 (1961).
[77] Y. Mitsui, Y. Iitaka, and M. Tsuboi, *Ibid., 24*, 15 (1967).
[78] J. M. Squire and A. Elliott, *Mol. Cryst. Liq. Cryst., 7*, 457 (1969).
[79] T. Yoshida, S. Sakurai, T. Okuda, and Y. Takagi, *J. Am. Chem. Soc., 84*, 3590 (1962).
[80] P. Dumas, N. Spassky, and P. Sigwalt, *Makromol. Chem., 156*, 55 (1972).
[81] N. Matsushima, K. Hikichi, A. Tsutsumi, and M. Kaneko, *Polym. J., 7*, 382 (1975).
[82] Y. Baba and A. Kagemoto, *Macromolecules, 10*, 458 (1977).
[83] H. Sakakihara, Y. Takahashi, H. Tadokoro, N. Oguni, and H. Tani, *Ibid., 6*, 205 (1973).
[84] H. Matsubayashi, Y. Chatani, H. Takodoro, P. Dumas, N. Spassky, and P. Sigwalt, *Ibid., 10*, 996 (1977).
[85] D. Grenier and R. E. Prud'homme, *J. Polym. Sci., Polym. Phys. Ed., 22*, 577 (1984).
[86] C. Lavallee and R. E. Prud'homme, *Macromolecules, 22*, 2438 (1989).
[87] Y. Ikada, K. Jamshidi, H. Tsuji, and S. H. Hyon, *Ibid., 20*, 904 (1987).
[88] G. L. Loomis, J. R. Murdoch, and K. H. Gardner, *Polym. Prepr. Am. Chem. Soc., Div. Polym. Chem., 31*(2), 55 (1990).
[89] G. L. Loomis and J. R. Murdoch, US Patent 4,719,246 (1988).
[90] G. L. Loomis and J. R. Murdoch, US Patent 4,766,182 (1988).
[91] G. L. Loomis and J. R. Murdoch, US Patent 4,800,219 (1989).
[92] G. L. Loomis and J. R. Murdoch, US Patent 4,902,515 (1990).
[93] G. L. Loomis and J. R. Murdoch, US Patent 4,981,696 (1991).
[94] H. Tsuji, F. Horii, S. H. Hyon, and Y. Ikada, *Macromolecules, 24*, 2719 (1991).
[95] H. Tsuji, S. H. Hyon, and Y. Ikada, *Ibid., 24*, 5651 (1991).
[96] H. Tsuji, S. H. Hyon, and Y. Ikada, *Ibid., 24*, 5657 (1991).
[97] H. Tsuji, S. H. Hyon, and Y. Ikada, *Ibid., 25*, 2940 (1992).
[98] H. Tsuji and Y. Ikada, *Ibid., 25*, 5719 (1992).
[99] H. Tsuji, F. Horii, M. Nakagawa, Y. Ikada, H. Odani, and R. Kitamaru, *Ibid., 25*, 4114 (1992).
[100] H. Tsuji and Y. Ikada, *Ibid., 26*, 6918 (1993).
[101] T. Okihara, M. Tsuji, A. Kawaguchi, K. Katayama, H. Tsuji, S.-H. Hyon, and Y. Ikada, *J. Macromol. Sci.—Phys., B30*, 119 (1991).

[102] K. Gardner, Unpublished Work.
[103] M. Spinu and K. H. Gardner, *PMSE (Am. Chem. Soc., Div. Polym. Mater: Sci. Eng.), 71*, 19 (1994).
[104] M. Spinu, US Patent 5,317,024 (1994).
[105] M. Bero, J. Kasperczyk, and Z. J. Jedlinski, *Makromol. Chem., 191*, 2287 (1990).